18th Conference on Aviation, Range, and Aerospace Meteorology, 2017, Seattle WA, poster 212.

Forecasting Hail Aloft

Donald McCann*
McCann Aviation Weather Research, Inc.

1. Introduction

Hailstorms can cause substantial damage to objects at the surface, such as crops, buildings, and automobiles. Since hail at the surface forms aloft in a thunderstorm's updraft, it is also a threat to flying aircraft. A hail encounter can pit airframe surfaces; especially vulnerable are soft material components such as nose cone radomes. Figure 1 shows hail damage to an Airbus A321 during ascent from Rio de Janeiro, Brazil, on 8 February 2015. Hailstones need not be large to pose danger because of a flying aircraft's high speed. Fortunately, most commercial aircraft have onboard radar which can easily detect hail. Nevertheless, aircraft are still being hail-damaged. A search on the website http://avherald.com found twenty-five hail strike accidents since 2010. The search engine found five cases between 2010 and 2013 but found six in 2014, eight in 2015, and six in 2016. The larger recent numbers suggest that more strikes may have occurred earlier but were limited by the search engine's capabilities. These reports happened worldwide, and many were in the tropics where surface hail reports are rare (Frisby and Sansom 1967). Some reports were more damaging than others, but none reported a hail size. Nevertheless, these cases are enough to create a data set large enough to document similarities about how hail forms aloft.

Hail grows in thunderstorms as updrafts loft small ice embryos upward to accrete supercooled liquid water and ice. Hailstones can grow larger if they fall through the supercooled cloud liquid water again. Brimelow et al. (2002) combined this hailstone growth model with a one-dimensional cloud model to predict hail size from sounding data. HAILCAST, as it is called, verifies well with ground hailstone observations over Canada and the United States (Jewell and Brimelow 2009). In order to predict ground hail size, HAILCAST must predict how hail grows aloft and could be an ideal model to analyze the aircraft hail strike cases gathered for this study.

Our goal is to create an operational worldwide hail size forecast for the aviation industry. To that end, we ran a similar-to-HAILCAST hail growth model on numerical weather model sounding forecasts at each case's hail report location. In every case, the model predicted only small hail at the reported flight level. These were soundings with substantial convective available potential energy (CAPE) that produced updrafts that quickly blew the tiny hail embryos through the cloud liquid water (CLW) accumulation zone. The hail never had a chance to get large.

Brimelow et al. (2002) found that if they shut off the updraft after a certain

* *Author's email:* don@mccannawr.com

time, the growing hailstone could fall through the CLW accumulation zone again and rapidly grow thus achieving observed large hail sizes. They limited the updraft time by a function of CAPE times wind shear which is also known as the energy-shear index (ESI). Unfortunately, this and other HAILCAST cloud model assumptions proved not to forecast details of hail formation very well in one well documented hail strike case. We reexamined the research to create a more complete sounding-coupled hail growth model that could apply to more thunderstorm situations. We then added the resultant hail growth algorithm to our programs that nowcast and forecast convective turbulence (McCann and Lennartson, 2014; 2015).

2. Hail Strike Database

We searched the *Aviation Herald* website (www.avherald.com) and found 25 hail strike cases. Additionally, Palmer (2013) noted that the doomed 2009 Air France 447 flight encountered small hail from sounds heard on the cockpit voice recorder minutes before it crashed. Table 1 lists the data. Hail strikes are truly a worldwide hazard. The only continents not represented are Australia and Antarctica. Australia is not immune to hailstorms; no hail encounters in the database were either due to chance or a very good air traffic control system. Nine reports were in the tropics defined as located between the Tropics of Cancer and Capricorn. All reports except Air France 447 were over continental locations.

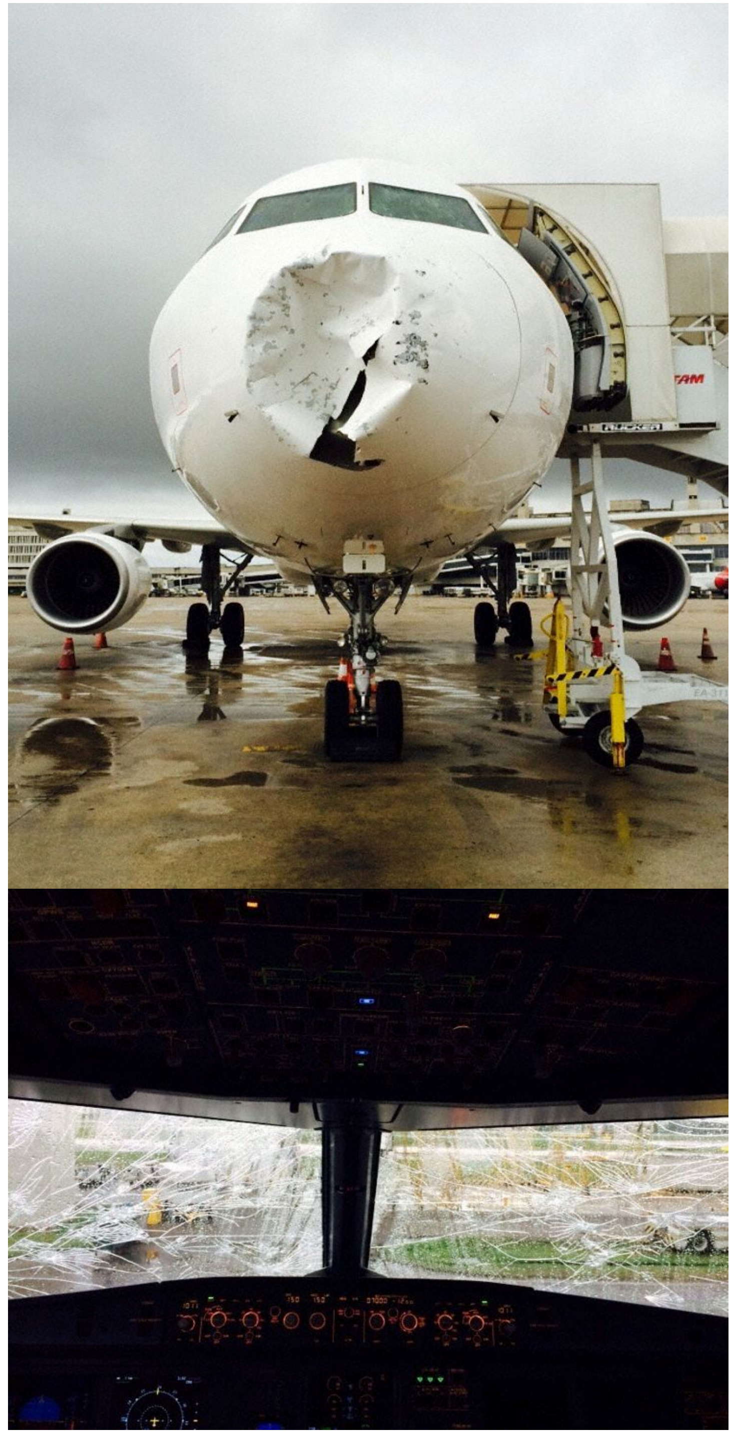

Figure 1. Hail damage to an Airbus A321 showing substantial damage to the airplane’s nose and windshield. (Source: http://avherald.com/h?article=48188170&opt=2304)

Date	Airline Flight	Location	Flight Level
1 Jun 09	Air France 447	03N 030W (central Atlantic Ocean)	360
3 Apr 10	Royal Jordanian 182	14N 101E (Thailand)	climb
14 Jul 11	Emirates 51*	48N 017E (Austria)	340
6 Sep 12	Egyptair 877	10N 008E (Nigeria)	descent
25 Apr 13	Far Eastern 191*	25N 111E (China)	320
12 Nov 13	Air France 443*	23S 043W (Brazil)	climb
27 Jan 14	Gol Linhas 1674*	14S 046W (Brazil)	climb
22 May 14	US Airways 768*	38N 075W (USA)	descent
27 May 14	Aigle Azur 232*	36N 006E (Algeria)	climb
8 Sep 14	Egyptair 859*	05N 031E (South Sudan)	descent
9 Sep 14	Air Europa 41*	34S 057W (Argentina)	250
8 Oct 14	Pakistan Intl 203*	31N 074E (Pakistan)	climb
8 Feb 15	TAM Linhas 3307*	22S 043W (Brazil)	climb
24 Feb 15	TAM Linhas 3793	25S 048W (Brazil)	300
17 Jun 15	Delta 159	48N 125E (China)	360
15 Jul 15	Jazz 8205	54N 123W (Canada)	160
27 Jul 15	American 88*	42N 118E (China)	260
8 Aug 15	Delta 1889*	40N 101W (USA)	340
19 Aug 15	Alitalia 2016	42N 012E (Italy)	climb
23 Aug 15	Interjet 5401	21N 098W (Mexico)	300
16 Apr 16	Druk 140*	26N 091E (India)	descent
9 Jul 16	China Southern 3483*	29N 104E (China)	descent
30 Jul 16	Air Canada 1159*	51N 114W (Canada)	descent
2 Aug 16	China Southern 3510*	36N 117E (China)	climb
26 Aug 16	Cathay Pacific 312*	22N 114E (China)	climb
11 Nov 16	South African 1113	29S 025E (South Africa)	descent

Table 1. Hail strike cases gathered for this study. Flight level is in hundreds of feet as per convention. The asterisk after the airline flight number indicates more substantial damage such as a cracked windshield or other airframe damage.

For each case we ordered archived numerical forecast model data just before the event. Cases over the United States and Canada used the Rapid Refresh model while the remainder used the Global Forecast System model. Both models are operational at the United States National Centers for Environmental Prediction. The forecast model time was that nearest to the report time.

3. An Initial Hail Growth Model

a. Hail Growth Equations

Although not a contemporary reference, Byers (1965) describes the hail growth process quite well. Hail can grow in one of two ways, wet and dry. Hailstones accrete CLW causing it to freeze and transfering heat to the developing hailstone. Wet hail growth occurs when the CLW accretion is so fast that the stone is unable to keep its outer part frozen. Sufficient heat transfer results in dry growth. These processes account for a hailstone's layered appearance when sliced open. Wet growth typically occurs at temperatures just below 0C when the hailstone is descending from cooler air aloft. Because the unfrozen liquid water can be shed from the falling hailstone, wet growth is almost always less than dry growth. We wanted the maximum hail size possible from our model, so we limited our analysis to dry growth only. Similarly, we don't consider hail melting. Byers (1965) describes the dry growth process

$$\frac{dD}{dt} = \frac{V_t(E_l\chi_l + E_i\chi_i)}{2\delta_r} \qquad (1)$$

where D is the hailstone diameter, V_t is the hailstone's terminal velocity, χ_l is the cloud liquid water and χ_i is the cloud ice, $E_l = 1.0$ and $E_i = 0.25$ are collection efficiencies for CLW and ice, respectively, and $\delta_r = 900$ kg m^{-3} is ice density. Equation (1) includes growth by ice accretion not considered by Byers but follows Brimelow (1999). Spherical hailstones fall at terminal velocities (m s^{-1}) given by

$$\begin{aligned} V_t &= 1 & D &< 500\mu m \\ V_t &= 1 + 6800(D - .0005) & 500\mu m &\le D < 1mm \\ V_t &= \sqrt{\frac{4gD\delta_r}{\rho C_d}} & D &\ge 1mm \end{aligned} \qquad (2)$$

where g is the acceleration of gravity, ρ is the air density, and $C_d = 0.6$, the hailstone's drag coefficient. Adiabatically, cloud liquid water forms in a layer by

$$\chi_l = \frac{3(\Delta z)\rho(\Gamma_d - \Gamma_m)C_p}{4L} + \frac{gr}{R_D T} \qquad (3)$$

where Δz is the layer thickness, Γ_d and Γ_m are the dry and moist adiabatic lapse rates, C_p is the specific heat of air at constant pressure, L is the latent heat, r is the parcel mixing ratio, R_D is the gas constant, and T is the parcel air temperature. Note that updraft speed is not in (3); upward moving parcels create the same CLW amount no matter how fast they move. Also note that precipitation processes to reduce CLW are not considered.

All cloud liquid water becomes ice at $T <$ -40C. Between -20C and -40C some CLW changes to cloud ice using the Vali and Stansbury (1965) depletion method. Their graphic solution approximately is

$$\begin{aligned} \chi_i &= 0 & T &> -20C \\ \chi_i &= \chi_l\left(\frac{T+20}{20}\right)^2 & -20C &< T < -40C \\ \chi_i &= \chi_l & T &< -40C \end{aligned} \qquad (4)$$

Because ice crystals do not stick to hailstones very well, in (1) only 25% of the cloud ice contributes to hail growth as opposed to CLW which sticks at 100%.

b. Hail Growth Implementation

Hailstones grow as they collect cloud liquid water and cloud ice. The hail growth model interpolates the numerical forecast model's environmental data to the point in question to create a sounding. The hail growth model finds the sounding's most unstable parcel then lifts it dry or moist adiabatically, as appropriate, into each layer aloft to compute the parcel's acceleration. Parcel accelerations are reduced for drag and entrainment by reducing the parcel's equivalent potential temperature (Θ_e) depending on the layer thickness and the environment's Θ_e.

Hail growth begins at the freezing level with an embryo. In HAILCAST the embryo size is 300 µm, but as will be shown in the next section, this was not large enough to fit the well documented case mentioned earlier. HAILCAST also begins growth at the lifting condensation level (LCL) with a 4 m s^{-1} initial updraft. If there is sufficient negative energy between the LCL and the level of free convection (LFC), the updraft may decelerate, halting embryo growth. To avoid the substantial initial updraft uncertainties, our model's initial growth is at the freezing level. The freezing level is almost always higher than the LFC; this ensures upward motion to carry the hail embryo upward. Hailstones grow in an atmospheric layer by equation (1) depending on the layer's CLW and cloud ice. The model grows hail in one second time increments. The hailstone rises or falls depending on its size (terminal velocity) and the parcel vertical velocity.

4. Developing a More Universal Hail Growth Model

In this section we examine HAILCAST's potential to identify hail aloft from soundings by comparing its results to the details of three hail strike cases. In these cases we know the altitude of the hail encounter and whether the hail was large or small. In the first case (Delta 1889) we also have radar and lightning coverage.

First, we propose a HAILCAST modification that overcomes a significant difficulty with its model concept. As stated earlier, HAILCAST uses an energy-shear index (CAPE times surface-6 km shear) to determine updraft longevity. Because hailstorm updrafts are typically very strong, growing HAILCAST hailstones often remain aloft. In order for hail to grow large, HAILCAST artificially stops the updraft to allow the hail to fall through the higher CLW collection zone. Conceptually, this means that large hail does not fall to the surface until the thunderstorm's dissipating stage. Also, it is questionable that the CLW will continue in place after the storm dissipates.

There is substantial research relating wind shear to storm type/longevity, i.e. isolated, multicell, or supercell (Weisman and Klemp, 1982), but Weisman and Klemp show that buoyancy alone does not increase a storm's lifetime. Moreover, a straightforward surface to 6 km wind shear does not account for the entire wind hodograph's shear. Weisman and Klemp (1984) show that a curved hodograph will enhance storm intensity more than a straight one, both with identical wind shear measured from beginning to end. Thus, the hodograph's arc length from the surface to 6 km will better measure the wind shear's enhancement potential. Furthermore, large hail has been observed in thunderstorms with origins above the surface. Thompson et al. (2007) define an effective bulk shear as the shear from the most unstable parcel level to a level between 6 km and the equilibrium level that accounts for the shear actually experienced by the thunderstorm. Therefore, we use the hodograph arc length from the most unstable parcel level to 6 km above that as our measure of shear.

Now, wind shear affects a storm's entrainment in two ways. First, entrainment is partially dependent on the storm's size. The core of larger storms is less affected by entrainment than in smaller storms. Storm numerical modeling studies cited above conclude that larger storms can develop with stronger wind shear. Second, studies of entrainment in wind shear suggest that most of the entrainment is on the storm's downshear side, leaving the upshear side relatively undiluted (Knupp and Cotton, 1985). Since entrainment reduces the storm's CLW, instead of halting the storm's updraft as in HAILCAST, we use an entrainment/wind shear relationship to reduce the CLW available for hailstone growth.

$$\chi_l = \chi_a\left(1-\frac{4}{S}\right) \qquad (5)$$

where χ_a is the adiabatic CLW computed from (3) and

$$S = \int_{z_0}^{z_0+6000}\left|\frac{d\mathbf{V}}{dz}\right| dz \qquad (6)$$

where S is the wind hodograph arc length from the most unstable parcel level (z_0) to 6 km above. The CLW is thus reduced to reasonable values, especially in tropical air masses in which the adiabatic CLW can often be greater than 7 g m^{-3}.

a. Delta 1889

On 7 August 2015, the Delta Airlines Airbus A320-200, flight 1889 from Boston MA to Salt Lake City UT encountered hail aloft at FL340[1] (10 363 m) near McCook NE about 0200 UTC (8 Aug). The hail cracked both windshields and damaged engines and the nose radome causing the radar to fail. The aircraft also encountered severe turbulence but reported no injuries. The crew diverted to Denver CO and landed successfully despite the poor windshield visibility problems.

The NEXRAD base reflectivity images in Figure 2 shows that the flight crew probably thought that there was room between the two thunderstorm complexes to fly. However, by the time they arrived, the hole closed, and the flight slammed into the storm's strongest part. Unfortunately, there was little the flight could do to avoid the storm. Both lightning data and echo top images (not shown) suggest that the storm that the flight encountered was multicelled with the culprit cell forming about 30 minutes prior. Subsequent radar images show that the storm weakened after the hail strike.

Figure 3 shows hailstone growth in green using original HAILCAST assumptions. The input sounding is from the 2 hour Rapid Refresh model forecast from 0000 UTC 8 Aug 2015, interpolated to Delta 1889's hail encounter position. It featured CAPE about 2400 J kg^{-1} and surface to 6 km wind shear about .00375 s^{-1} yielding an energy shear index about 9 m^{-2} s^{-3}, well

[1] "FL" is the flight level as measured on a standard atmosphere altimeter in hundreds of feet, in this case 34 000 ft.

above the 5 m^{-2} s^{-3} threshold for a HAILCAST 60 minute updraft longevity. The storm updraft after the entrainment adjustment maximizes about 38 m s^{-1}, much less than the 69 m s^{-1} adiabatic updraft. Hailstones only grow to about 1 mm as they are swept upward into the storm's upper reaches in 7 minutes and remain there for the final 53 minutes. Obviously, Delta 1889 encountered much larger hail. Surface golf ball size hail (4.5 cm) was reported about an hour earlier in another nearby storm, and the NEXRAD maximum hail size algorithm (not shown, Witt et al. 1998) indicated greater than 5 cm surface hail with this cell. Hail aloft was larger than the surface values because it would not have melted. HAILCAST failed to forecast the observed hail.

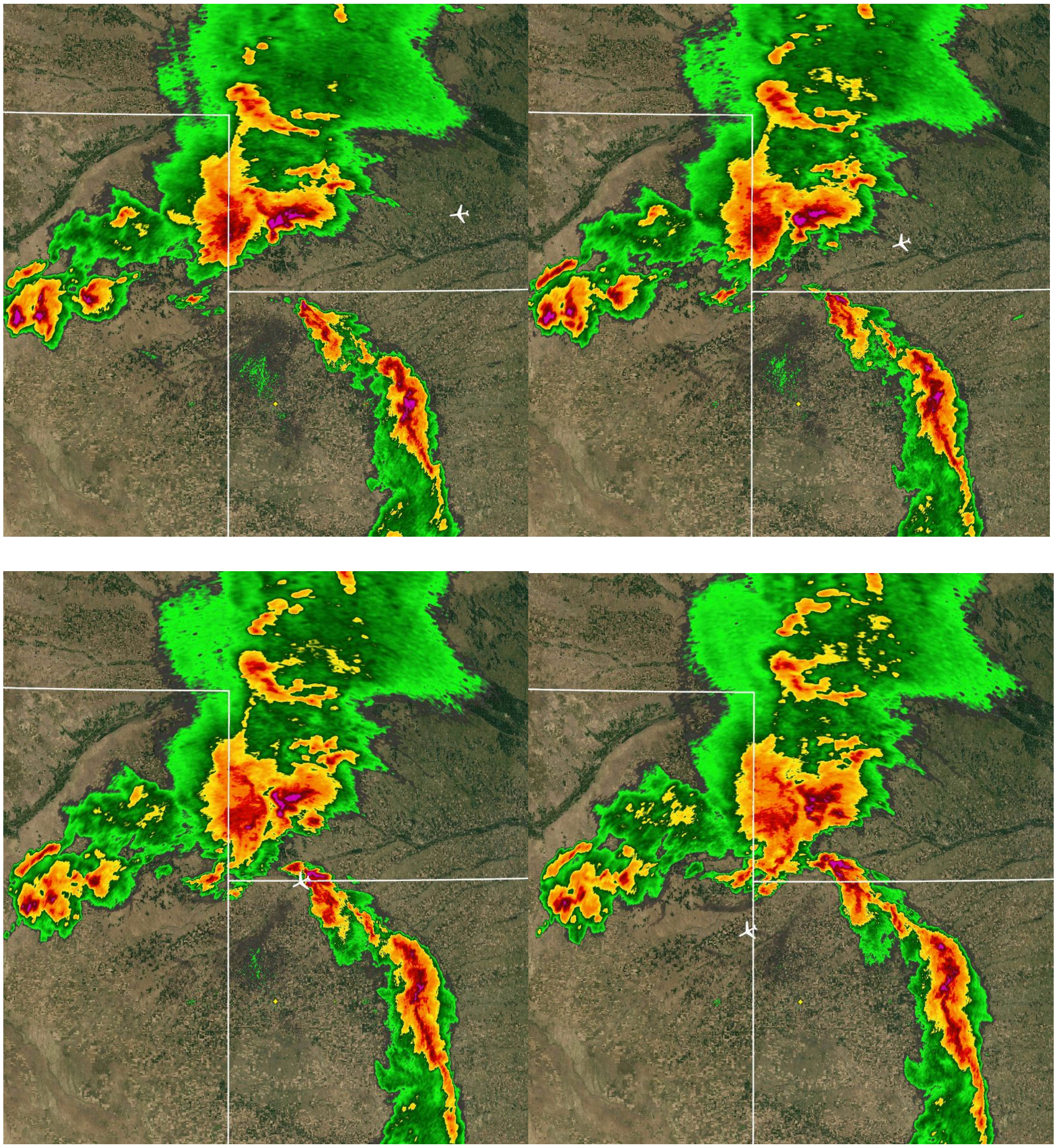

Figure 2. Composite NEXRAD base reflectivity images from 8 Aug 2015 approximately 0145-0205 UTC. Aircraft symbol shows the position of Delta 1889. Images are from Ostro (2015).

So what adjustments should we make? Actually, only one is necessary. Hail begins as an embryo created previously by weaker updrafts (Knight and Knight, 1970). An embryo can be graupel, a frozen raindrop, or a melting ice crystal, to list more common sources. HAILCAST assumes a 300 µm embryo which is so small that hailstones do not grow to significant size. Knight and Knight assert that hail embryos may be as large as 1 cm. We can manipulate the resulting hail if we vary the initial embryo size**.** The goal is to predict hail size large enough to cause damage to Delta 1889 at the altitude flown (FL340) within 30 minutes.

Figure 3 shows the hail growth with a 3.5 mm starting embryo. Hailstones rise to just less than 11 000 m, and in less than 20 minutes hail grows to 3.7 cm as they fall through FL340. Note that this was with less CLW than original HAILCAST because of the equation (5) modifications. Also shown are the hail growth results for a 3 mm embryo. It grows to about 2 cm diameter as it rises to above 12 000 m, but, similar to the HAILCAST hail, it never falls back into the CLW collection zone. Results for a 4 mm embryo show a rise only to about 10 000 m before falling.

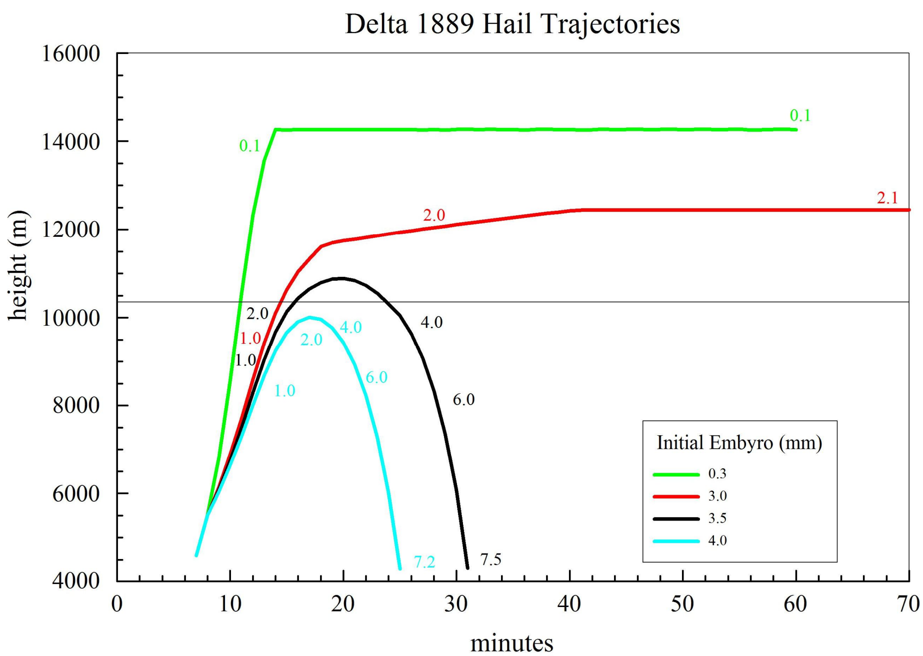

Figure 3. Hail trajectories for the Delta 1889 case with various initial embryo sizes. The small numbers are the approximate hail sizes (cm) colored the same as the corresponding trajectory curve. The numbers are located near the time/altitude that the hail reaches that size. The horizontal line is the flight altitude of Delta 1889.

The final hail size for embryos at least 3.5 mm at the melting level is approximately 7.5 cm. Considering that the melting level was approximately 4 300 m above ground level, the observed 5 cm surface hail is consistent with our results. While the initial embryo size makes a difference in the hailstone evolution, the final hail size is not very dependent on initial embryo size, as long as it is large enough. This initial embryo size is slightly more than an order of magnitude larger than that in HAILCAST.

b. Air France 447

Air France 447 tragically disappeared into the Atlantic Ocean on the evening of 31 May 2009. Searchers found the Airbus A330-200 wreckage nearly 2 years later 12 800 feet below sea level. They found the Flight Data Recorder (FDR) and the Cockpit Voice Recorder (CVR) surprisingly intact. In detail, Palmer (2013) describes the accident investigation. Flying at FL360 in tropical convection, Air France 447 experienced light-moderate turbulence. As the flight encountered an updraft, a sound typical of ice crystals hitting the fuselage was heard on the CVR. The ice clogged the pitot tubes that indicate the air speed. The unreliable air speed triggered a chain of events leading to the aircraft's loss of control.

Pitot tube diameters are approximately 1 cm. Ice crystal diameters are typically 1 mm or less. On the other hand, graupel diameters are larger, 1-3 mm diameter. Given that the ice could be heard on the CVR, Air France 447 might have encountered graupel which, intuitively, would be more likely to clog the pitot tube. We ran our hail growth model on the three hour GFS 0000 UTC 1 June 2009 model. Figure 4 shows our hailstone growth model with a 3.5 mm embryo. Hail grows too fast and begins falling before it reaches 7 km.

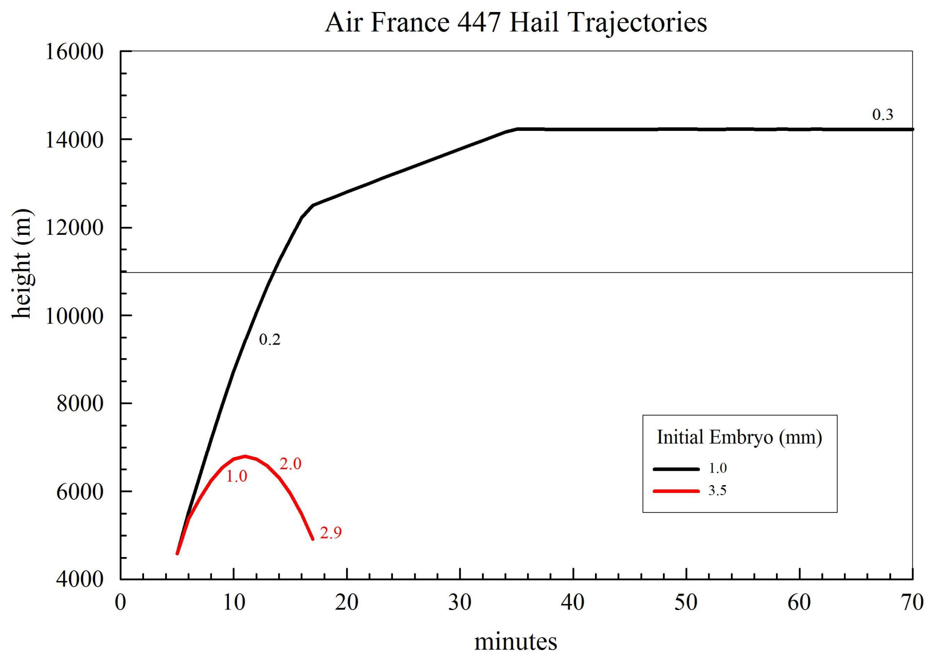

Figure 4. Hail trajectories for the Air France 447 case with two initial embryo sizes. The 3.5 mm initial embryo also assumed a continental cloud liquid water profile while the 1.0 mm initial embryo assumed a marine cloud liquid water profile. The small numbers are the approximate hail sizes (cm) colored the same as the corresponding trajectory curve. The numbers are located near the time/altitude that the hail reaches that size. The horizontal line is the flight altitude of Air France 447.

It is obvious that if hail embryos start large, 3.5 mm in this case, hail will only grow even larger, too large for that likely observed by Air France 447. Therefore, hail embryos should be smaller. Because there is no research on hail embryo size over marine environments, we assume that they must be no larger than about 1 mm.

However, vertical CLW profiles in convection over oceanic areas are substantially different from continental areas. Andraea et al. (2004) show that in marine convection, CLW forms in large droplets because of larger condensation nuclei. This causes the droplets to enlarge to precipitation size and fall from updraft earlier than in continental convection. Ackerman (1963) even observed low CLW aloft in hurricanes. Andraea et al. also report hail aloft in smoky continental environments with small condensation nuclei.

Furthermore, we see that almost all the Table 1 hail strike cases are continental. Only marine-convection-encountered Air France 447 was not damaged by hail. We are aware of several other cases on file in which the oceanic aircraft encountered severe turbulence but not hail. All the evidence points to large hail as being almost exclusively continental.

Therefore, we adjusted our hail growth model for oceanic areas by 1) reducing the initial hail embryo to 1 mm from the continental 3.5 mm, and 2) reducing CLW by accounting for the collision-coalescence process that forms precipitation lower in the updraft.

$$\chi_l = \chi_{l_i}\left(1 - \frac{v_t(1mm)}{w(z)}\right) \quad z > z_{lcl} + 1km \tag{7}$$

where χ_{li} is the integrated CLW from (5) and $v_t = 6$ m s^{-1} is the terminal velocity of a 1 mm raindrop. This procedure is invoked at updraft levels 1 km and higher above the LCL. Because collision-coalescence seldom happens in continental storms, we only apply this method over maritime regions.

The maximum CLW reduced to 0.9 g m^{-3} after the collision-coalescence adjustment from 4.2 g m^{-3} before. After adjustment, the Air France 447 hail only grows to 2.4 mm at FL360 (Fig. 4), a size near that probably observed.

c. *Emirates 51*

On 14 July 2011, an Emirates Airbus A330-200 enroute at FL340 from Dubai, United Arab Emirates, to Munich, Germany, encountered hail south of Vienna, Austria. The hail cracked the windshield and damaged the nose cone paint. The plane diverted to Prague, Czech Republic.

Figure 5 shows that in our model the hail grew to about 1 cm at FL340 but could not grow enough to fall back into the CLW collection zone to grow much larger. Brimelow et al. (2002) noted that if updrafts were too strong, the hail would stay aloft in the storm's anvil. In this case, the maximum updraft was 50 m s^{-1}. When we reduced the updraft speed to a maximum 38 m s^{-1}, the hail altitude only reached 10 800 m, as not only could the rising hail grow larger in the slower updraft but also it could grow large enough to descend. The hail grew to about 4 cm at FL340, a size more likely to cause the damage that the aircraft sustained.

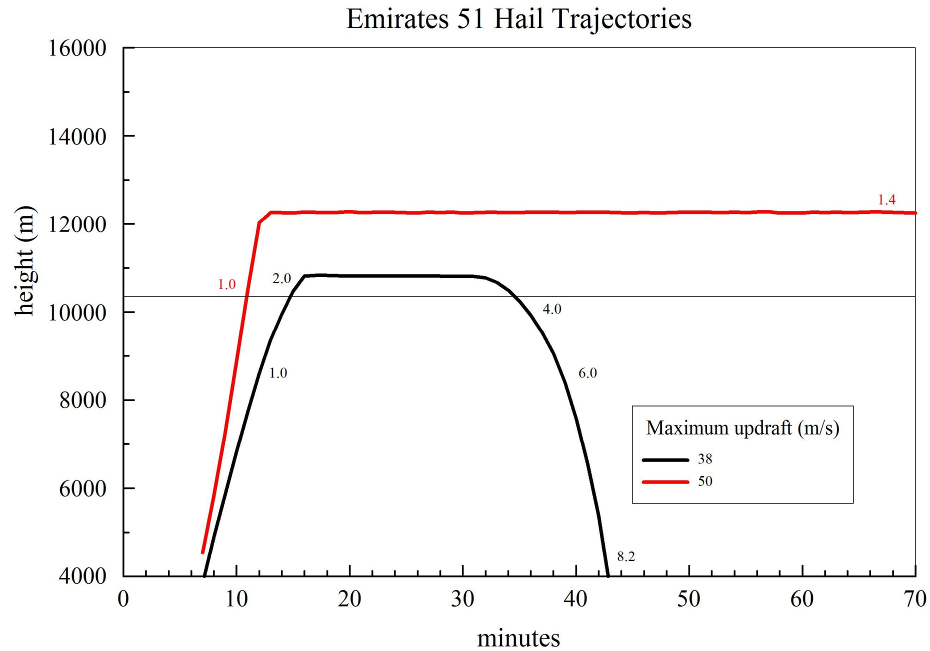

Figure 5. Hail trajectories for the Emirates 51 case with two maximum updraft speeds. The small numbers are the approximate hail sizes (cm) colored the same as the corresponding trajectory curve. The numbers are located near the time/altitude that the hail reaches that size. The horizontal line is the flight altitude of Emirates 51.

It is obvious that hail will not grow to a large size in an excessively fast updraft speed. Also obvious is that in a thunderstorm with a very fast maximum updraft, there will be slower speeds that will support large hail. Therefore, our hail growth model limits the maximum updraft speed to 38 m s^{-1}.

5. Hail Potential Forecasts

We applied our improved hail growth model to all the Section 2 hail strike cases. Table 2 shows the results. Only one case did the improved hail growth model not forecast hail at the flight level (Jazz 8205, 15 Jul 2015) because the forecast 16 m s^{-1} updrafts could support hail growth only as high as 3300 m (11 000 ft). The median hail size for the 17 aircraft with substantial damage (labeled with asterisks in Table 2) was 4.9 cm while the median size for the 9 lesser damaged aircraft was 2.2 cm. This indicates some skill in forecasting hail size aloft.

Date	Airline Flight	Flight Level	Hail(cm)	Max Hail(cm)
1 Jun 09	Air France 447	360	0.2	0.3
3 Apr 10	Royal Jordanian 182	climb	5.1	5.1
14 Jul 11	Emirates 51*	340	3.9	8.1
6 Sep 12	Egyptair 877	descent	5.8	5.8
25 Apr 13	Far Eastern 191*	320	3.6	7.5
12 Nov 13	Air France 443*	climb	4.1	4.1
27 Jan 14	Gol Linhas 1674*	climb	7.0	7.0
22 May 14	US Airways 768*	descent	6.3	6.3
27 May 14	Aigle Azur 232*	climb	4.1	4.1
8 Sep 14	Egyptair 859*	descent	5.7	5.7
9 Sep 14	Air Europa 41*	250	2.7	3.4
8 Oct 14	Pakistan Intl 203*	climb	3.9	3.9
8 Feb 15	TAM Linhas 3307*	climb	6.8	6.8
24 Feb 15	TAM Linhas 3793	300	0.8	1.9
17 Jun 15	Delta 159	360	2.2	6.3
15 Jul 15	Jazz 8205	160	0.0	0.6
27 Jul 15	American 88*	260	3.8	5.0
8 Aug 15	Delta 1889*	340	3.7	7.5
19 Aug 15	Alitalia 2016	climb	5.6	5.6
23 Aug 15	Interjet 5401	300	2.4	4.6
16 Apr 16	Druk 140*	descent	8.3	8.3
9 Jul 16	China Southern 3483*	descent	3.2	3.2
30 Jul 16	Air Canada 1159*	descent	4.9	4.9
2 Aug 16	China Southern 3510*	climb	5.0	5.0
26 Aug 16	Cathay Pacific 312*	climb	5.7	5.7
11 Nov 16	South African 1113	descent	0.7	0.7

Table 2. Hail forecasts for the Table 1 cases. For climb or descent cases the maximum hail size is the forecast hail size. For hail strikes at a specific flight level, the size is that predicted by the hail growth model. As in Table 1, the asterisk after the airline flight number indicates more substantial damage such as a cracked windshield or other airframe damage.

The improved hail growth is implemented in Schneider Electric's two aviation specific thunderstorm forecast algorithms. VVTURB (McCann 1999) provides convective forecasts based on the generally-accepted ingredients-based forecast techniques used by most human forecasters, that is, finding zones with substantial potential instability and a mechanism that will lift potentially unstable parcels to their level of free convection.[2] VVTURB computes updraft velocities which are correlated to turbulence at every level in numerical models. The hail growth model uses these updraft velocities to compute hail size. Figure 6 shows the maximum hail size aloft for the Delta

[2] VVTURB was known as VVSTORM until 2012 when the algorithm's name changed.

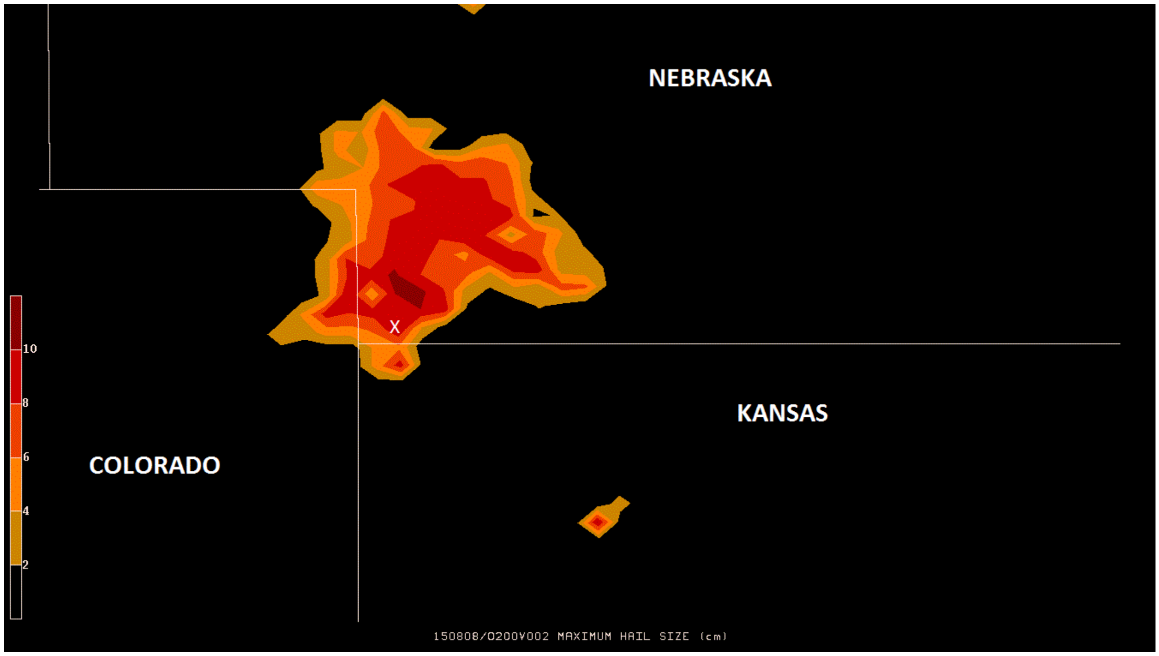

Figure 6. Maximum hail size aloft forecast computed by VVTURB from the 0000 UTC 8 August 2015 Rapid Refresh model 2 hour forecast. The forecast verifies about the time of the Delta 1889 hail strike which is marked by the "X."

1889 case in Section 4a. We could create altitude-specific hail size forecasts, but because there is already much uncertainty (discussed below) that we felt that such specificity would not be of much value. VVSTORM is Schneider Electric's other convection forecast algorithm. VVSTORM computes potential storm updrafts, not considering lifting mechanisms. Schneider Electric's new 0-1 hour nowcast (McCann and Lennartson 2015) locates the actual updrafts with observed lightning. Lightning intensity modifies VVSTORM 's updraft forecasts. These observed thunderstorms are forecast for the next hour, and the resulting turbulence for all altitudes computed. Similar to VVTURB, the nowcast calculates maximum hail size from the updraft forecasts. Figure 7 shows the maximum hail size nowcast for the Alitalia 2016 case on 19 August 2015.

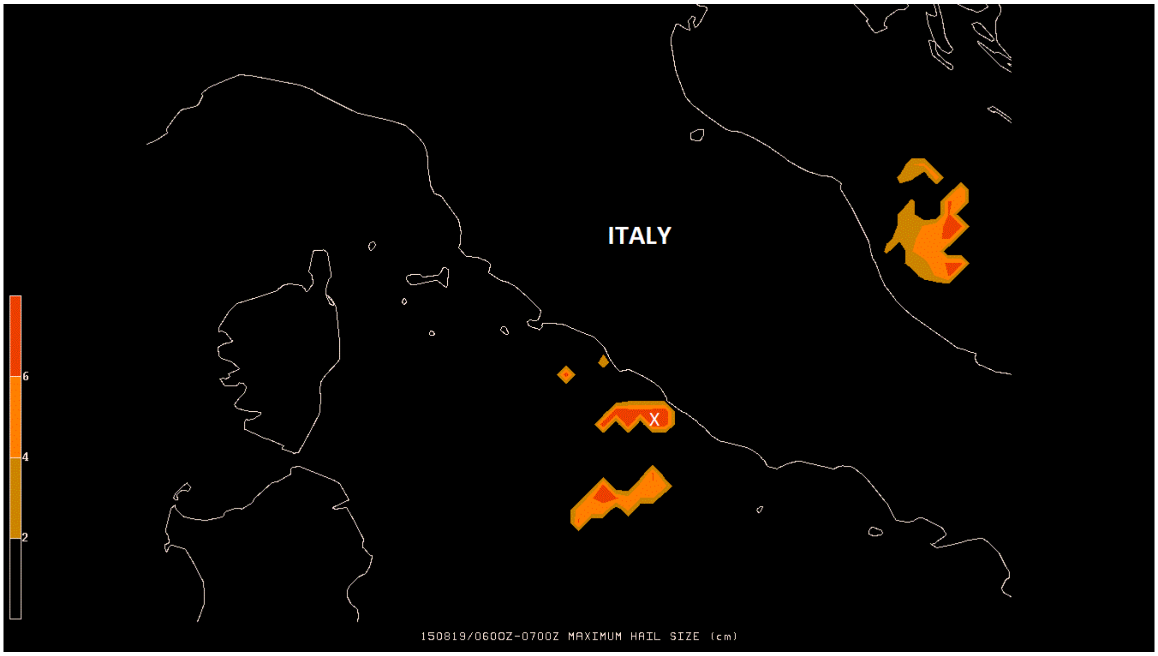

Figure 7. Maximum hail size aloft nowcast . The nowcast is for the period 0600-0700 UTC 19 August 2015. The Alitalia 2016 flight encountered hail about 0625 UTC which is marked by the "X."

6. Limitations

The previous sections presented a comprehensive methodology to forecast/nowcast hail size. Missing, of course, is a discussion of the false alarm rate which, as with forecasts of other rare severe weather phenomena, is difficult to measure. To be sure, for several reasons these hail size forecasts/nowcasts will overforecast events. First, as was shown above, hail evolution is very dependent on embryo size. More importantly, embryos must exist before large hail forms. Even if embryo-forming pre-existent updrafts exist, they must be positioned to feed embryos to the primary updraft. This is the primary reason why hail is so rare in thunderstorms. Second, the hail growth model assumes that hailstones reaching the critical falling size descend through the maximum cloud liquid water zone. This will only happen with a proper configuration of the hailstorm's internal flow. If descending hailstones fall through lesser cloud liquid water, they will be smaller. On the other hand, hailstones may recycle more than once through CLW zones and grow even larger. We estimate that, given that our hail growth model only allows for hail to ascend and descend once, the largest hail would be 10-12 cm. To reach near record 20 cm diameter hail, stones would have to move up and down more than once. Third, the largest hail occurs near the freezing level because hailstones begin to melt at lower altitudes. In typical environments that support hail, the freezing level is about 3000-5500 m (FL100-FL180) mean sea level. Most commercial aircraft fly much higher, so if they run into hail while cruising, it will likely be smaller.

Our goal is to create hail forecasts from numerical model forecasts. Even today's high resolution model forecasts do not have sufficient detail to resolve the many hailstorm subtleties. Nevertheless, there is sufficient information, even in medium resolution models, to compute a reasonable estimate of maximum hail size potential. Since we established that hail aloft is a worldwide hazard and not limited to typical severe storm environments, for now, users should accept these limitations to receive the forecast benefits.

7. Conclusions

Hail aloft remains a significant aviation hazard today as our database of recent hail strikes demonstrates. Modern jet aircraft have onboard radar, so one can surmise that it might be a lack of money or training that is contributing to the problem. However, inadvertent hail strikes occur to both large and small commercial airline operations, so the problem is not limited by poor resources but appears to be minimal situational awareness. Give an aircraft adequate warning, and it is less likely that it will be hail struck. That is our motivation for developing hail aloft forecasts.

We began with basic hail growth equations using the Brimelow et al. (2002) HAILCAST model but found HAILCAST had significant shortcomings when applied to the worldwide hail strikes cases in our database. Foremost was that damaging hail aloft is not limited to supercell environments. Certainly, in supercell environments hail is more likely, but any environment with adequate moisture that can be lifted aloft to form supercooled cloud liquid water aloft can support hail. We actually had to add processes such as more entrainment and precipitation fallout to limit the cloud liquid water development to reasonable values.

The result is a more robust hail growth model that can be implemented worldwide on numerical forecast model output. Its performance on the cases in our database is adequate. We have added it to Schneider Electric's forecast and nowcast algorithms so users will be more aware of any potential hail aloft in their paths.

Acknowledgements

I would like to thank Steve Corfidi and Dan Lennartson for their comments on this paper's initial draft. They helped make the paper stronger. This research is funded by Schneider Electric.

REFERENCES

Ackerman, B., 1963: The distribution of liquid water in hurricanes. National Hurricane Research Project Report No. 62. Available at http://www.aoml.noaa.gov/general/lib/TM/NHRP_62_1963.pdf

Andraea, M.O., D. Rosenfeld, P. Artaxo, A. A. Costa, G. P. Frank, K. M. Longo, M. A. F. Silva-Dias, 2004: Smoking rain clouds over the Amazon. *Science*, **303**, 1337-1342.

Brimelow, J. C., 1999: Numerical modelling of hailstone growth in Alberta storms. M.S. thesis, Dept. of Earth and Atmospheric

Sciences, University of Alberta, 153 pp.

Brimelow, J.C., G.W. Reuter, and E.R. Poolman, 2002: Modeling maximum hail size in Alberta thunderstorms. *Wea. Forecasting*, **17**, 1048–1062.

Byers, H.R., 1965: *Elements of Cloud Physics*, University of Chicago Press, Chicago.

Frisby, E.M. and H.W. Sansom, 1967: Hail incidence in the tropics. *J. Appl. Meteor.,* **6**, 339-354.

Jewell, R. and J.C. Brimelow, 2009: Evaluation of Alberta hail growth model using severe hail proximity soundings from the United States. *Wea. Forecasting*, **24**, 1592-1609.

Knight, C.A. and N.C. Knight, 1970: Hail embryos. *J. Atmos. Sci.*, **27**, 659-666.

Knupp, K.R. and W.R. Cotton, 1985: Convective cloud downdraft structure: An interpretative study. *Rev. of Geophysics*, **23**, 183-215.

McCann, D.W., 1999: VVSTORM – Convection diagnosed from numerical models. *Proc. Eighth Conf. on Aviation, Range, and Aerospace Meteorology*, Dallas TX, Amer. Meteor. Soc., 240-243.

McCann, D.W. and D.W. Lennartson, 2014: Integrated turbulence forecasts. Fourth Aviation, Range, and Aerospace Meteorology Special Symposium. Atlanta, GA, paper 4.4, https://ams.confex.com/ams/94Annual/webprogram/Paper230413.html

McCann, D.W. and D. Lennartson, 2015: The New Turbulence Nowcast from Schneider Electric. Seventeenth Aviation, Range, and Aerospace Meteorology Conference, Phoenix AZ, paper 6.5, https://ams.confex.com/ams/95Annual/webprogram/Paper262145.html

Ostro, S., 2015: Meteorological analysis of flight diverted by hail damage. http://www.wunderground.com/blog/stuostro/comment.html?entrynum=33

Palmer, B., 2013: *Understanding Air France 447*, ISBN: 978-0-9897857.

Thompson, R.L., C.M. Mead, and R. Edwards, 2007: Effective Storm-Relative Helicity and Bulk Shear in Supercell Thunderstorm Environments. *Wea. Forecasting*, **22**, 102-115.

Vali, G., and E.J. Stansbury, 1965: Time-dependant characteristics of the heterogeneous nucleation of ice. Sci. Rept.. MW-4 1. Montreal, McGill University, 31 pp.

Weisman, M. L., and J. B. Klemp, 1982: The dependence of numerically simulated convective storms on vertical wind shear and buoyancy. *Mon. Wea. Rev.,* **110,** 504–520.

Weisman, M. L., and J. B. Klemp, 1984: The structure and classification of numerically simulated convective storms in directionally varying wind shears. *Mon. Wea. Rev*., **112**, 2479–2498.

Witt, A., M.D. Eilts, G.J. Stumpf, J.T. Johnson, E.D. Mitchell, and K.W. Thomas, 1998: An enhanced hail detection algorithm for the WSR-88D. *Wea. Forecasting*, **13**, 286-303.